Investigating the Stability of Mass Transfer in Neutron Star–helium White Dwarf Binaries

Chen, Hai Liang; Tauris, Thomas M.; Chen, Xuefei; Han, Zhanwen

Published in:
Astrophysical Journal

DOI (link to publication from Publisher):
10.3847/1538-4357/ac6608

Publication date:
2022

Document Version
Publisher's PDF, also known as Version of record

The Astrophysical Journal, 930:134 (7pp), 2022 May 10 https://doi.org/10.3847/1538-4357/ac6608

Investigating the Stability of Mass Transfer in Neutron Star–helium White Dwarf Binaries

Hai-Liang Chen[1], Thomas M. Tauris[2], Xuefei Chen[1,3], and Zhanwen Han[1,3]
[1] Yunnan Observatories, Chinese Academy of Sciences (CAS), Kunming 650216, People's Republic of China; chenhl@ynao.ac.cn
[2] Department of Materials and Production, Aalborg University, Skjernvej 4A, DK-9220 Aalborg Øst, Denmark
[3] University of the Chinese Academy of Sciences, Yuquan Road 19, Shijingshan Block, 100049, Beijing, People's Republic of China
Received 2022 March 10; revised 2022 April 6; accepted 2022 April 7; published 2022 May 12

Abstract

Neutron star–helium white dwarf (NS+He WD) binaries are important evolutionary products of close-orbit binary star systems. They are often observed as millisecond pulsars and may continue evolving into ultracompact X-ray binaries (UCXBs) and continuous gravitational wave (GW) sources that will be detected by space-borne GW observatories, such as LISA, TianQin, and Taiji. Nevertheless, the stability of NS+He WD binaries undergoing mass transfer has not been well studied and is still under debate. In this paper, we model the evolution of NS+He WD binaries with WD masses ranging from 0.17–0.45 $M_{\odot}$, applying the detailed stellar evolution code MESA. Contrary to previous studies based on hydrodynamics, we find that apparently *all* NS+He WD binaries undergo stable mass transfer. We find for such UCXBs that the larger the WD mass, the larger the maximum mass-transfer rate and the smaller the minimum orbital period during their evolution. Finally, we demonstrate numerically and analytically that there is a tight correlation between WD mass and GW frequency for UCXBs, independent of NS mass.

Unified Astronomy Thesaurus concepts: Compact binary stars (283); X-ray binary stars (1811); Neutron stars (1108); White dwarf stars (1799); Gravitational wave sources (677)

1. Introduction

Among the common products of X-ray binaries are neutron star–white dwarf (NS+WD) systems, which are important for studies of close binary evolution (e.g., Tauris & van den Heuvel 2023). Due to gravitational wave (GW) radiation in NS+WD binaries with short orbital periods, the WD may overfill its Roche lobe and the systems become semidetached within the age of the Universe. If their mass transfer is dynamically stable, they evolve into long-lived ultracompact X-ray binaries (UXCBs; Nelson et al. 1986). Because of their short orbital periods, their GW signals can be detected by space-borne low-frequency GW observatories like LISA (Amaro-Seoane et al. 2022), TianQin (Luo et al. 2016), and Taiji (Ruan et al. 2020). If their mass transfer is unstable, the systems eventually merge and may give rise to transient events (e.g., Fernández et al. 2019; Zenati et al. 2019, 2020; Bobrick et al. 2022), producing exotic objects such as Thorne-Żytkow–like objects (Paschalidis et al. 2011), long gamma-ray burst (King et al. 2007), or fast radio burst (Katz 2021).

The stability of mass transfer in NS+He WD binaries, however, is still a topic of debate and could strongly influence the predicted number of UCXBs as GW sources. In earlier studies, it was common to use a critical WD mass, or a threshold mass ratio between the WD and the NS, to predict the stability of the mass transfer. Some studies (e.g., Verbunt & Rappaport 1988; Paschalidis et al. 2009; Yungelson et al. 2002; van Haaften et al. 2012; Yu et al. 2021) adopted semi-analytic methods to model the evolution of NS+WD binaries and showed that the critical WD mass is approximately 0.37–1.25 $M_{\odot}$, mainly depending on the stability criteria of mass transfer. However, in these studies, the detailed structure of the WD was not considered and the WD was assumed to be completely degenerate. Given that He WDs usually have an outer layer of nondegenerate hydrogen, possibly still relatively hot at the moment mass transfer is initiated, such semi-analytic studies may not be realistic, as demonstrated by, e.g., Istrate et al. (2014b, 2016), Sengar et al. (2017), and Tauris (2018).

Bobrick et al. (2017) carried out hydrodynamic simulations of mass transfer for NS+WD binaries. They found that disk winds appear during the mass-transfer process and measured the specific angular momentum loss of the disk winds. By combining the results of hydrodynamic simulations with a semi-analytic long-term evolution model, they found that the critical WD mass is only 0.20 $M_{\odot}$, i.e., much smaller than the results from other studies. They also found that the critical WD mass strongly depends on the angular momentum loss from the binary system.

Motivated by the work of Sengar et al. (2017) and Chen et al. (2021), who modeled the detailed structure of He WDs in UCXBs (produced as NS companion remnants in low-mass X-ray binaries (LMXBs)), we model here the evolution of mass transfer in NS+He WD binaries with a range of different WD masses using the stellar evolution code Modules for Experiments in Stellar Astrophysics (MESA; Paxton et al. 2011, 2013, 2015, 2018, 2019).

The remainder of this paper is organized as follows. In Section 2, we introduce the code and the assumptions we adopt for our simulations. In Section 3, we present the results we obtained. In Section 4, we discuss uncertainties and their influence on our simulations. In addition, we discuss general properties of UCXBs as GW sources. Finally, we summarize our conclusion in Section 5.

2. Method and Assumptions

2.1. Initial He WD Models

It is known that NS+He WD binaries in the Galactic disk can be produced via either (i) stable mass transfer (Roche-lobe

Table 1
Parameters of Simulated NS+He WD Binaries

M_2 ($M_\odot$)	$P_{\rm orb}$ (days)	$\log_{10}(T_{\rm c}/{\rm K})$	$\log_{10}(T_{\rm eff}/{\rm K})$	$P_{\rm orb}^{\rm RLO}$ (days)	$\log_{10}(T_{\rm c}^{\rm RLO}/{\rm K})$	$\log_{10}(T_{\rm eff}^{\rm RLO}/{\rm K})$	$P_{\rm min}$ (minutes)
0.17	0.30	6.995	3.88	0.0051	6.898	3.79	4.79
0.21	0.20	6.992	3.93	0.0038	6.934	3.88	3.78
0.25	0.05	6.996	3.96	0.0029	6.994	3.96	3.08
0.30	0.05	6.991	3.98	0.0022	6.989	3.98	2.45
0.35	0.02	6.998	4.01	0.0017	6.997	4.01	2.04
0.40	0.02	6.994	4.02	0.0014	6.994	4.01	1.72
0.43	0.02	6.997	4.03	0.0013	6.997	4.03	1.56
0.45	0.02	6.997	4.03	0.0012	6.997	4.03	1.48

Note. The first column is the initial WD mass. Columns 2–4 are the initial model values of orbital period, central temperature, and effective temperature. Columns 5–7 are the same values at the onset of RLO. Column 8 is the minimum orbital periods during their UCXB evolution.

overflow (RLO)) onto an NS from a main-sequence or a red-giant star companion (e.g., Tauris & Savonije 1999; Istrate et al. 2014a; Chen et al. 2021), or (ii) through common envelope (CE) evolution that ejects the hydrogen-rich envelope of the companion star (e.g., Tutukov & Yungelson 1993; Ivanova et al. 2013). In addition, in globular clusters, they can also form via exchange encounter events (e.g., Ivanova et al. 2008). The NS+He WD systems that are produced via stable RLO, and evolve to become semidetached UCXBs within the age of the Universe, have He WD masses $<0.17\,M_\odot$ (Sengar et al. 2017; Tauris 2018; Chen et al. 2021). UCXBs with larger initial WD masses can only be produced via the CE channel, or in an exchange encounter event in a dense stellar environment.

Because it is difficult to model in detail the outcome of a CE process or an exchange encounter event, we apply here a method where we first produce a range of He WD models with different masses between 0.17 and $0.45\,M_\odot$ via stable RLO in LMXBs with different initial orbital periods (see below), and then we artificially pair these He WDs in new tight orbits with an NS such that the WDs will be forced to fill their Roche lobe and initiate mass transfer. This approach allows us to study the stability of the RLO in NS+He WD (UCXB) systems.

We start by computing the evolution of a grid of LMXBs with the MESA code following the method described by Istrate et al. (2014a). The initial donor in this grid is assumed to be a ZAMS star with a mass of $1.2\,M_\odot$. The initial orbital period ranges between 1.0 and 600 days. The initial NS mass is assumed to be $1.30\,M_\odot$ (but is irrelevant here in the LMXB stage that is only needed to produce WD models for the next UCXB stage). After the LMXB stage, we extract and save the He WD model when its central temperature is $\sim 10^7$ K. The WD masses and their central and surface temperatures are listed in Table 1.

Afterward, in the second stage, we take these WD models as the initial WD models of NS+He WD binaries in our UCXB simulations. Compared with NS+He WD binaries produced from CE evolution, the He WDs may have different temperatures and residual hydrogen envelope masses. However, as we shall see, these factors have little impact on our results.

2.2. Evolutionary Models of NS+He WD Binaries

To obtain realistic mass-transfer rate evolution for NS+He WD binaries, we evolve an NS accretor and a He WD companion with the star_plus_point_mass test suite of MESA code (version 12115). We thus take the NS as a point mass and assume its mass to be $1.30\,M_\odot$. The initial orbital periods and WD properties, as well as those at the subsequent onset of RLO, are listed in Table 1. To secure approximately similar central WD temperatures in all our models (and to help the code to smoothly converge), the initial orbital periods are chosen so that the He WDs do not become too cold before they overfill their Roche-lobe radii.

In our calculation, two kinds of angular momentum loss mechanisms are considered: GW radiation and angular momentum loss due to mass loss. The following formula is adopted to compute the angular momentum loss due to GW radiation (Landau & Lifshitz 1971):

$$\frac{dJ_{\rm gw}}{dt} = -\frac{32}{5}\frac{G^{7/2}}{c^5}\frac{M_{\rm NS}^2 M_2^2 (M_{\rm NS}+M_2)^{1/2}}{a^{7/2}}, \quad (1)$$

where G and c are the gravitational constant and the speed of light in vacuum, respectively; a is the binary separation; $M_{\rm NS}$ and M_2 are the masses of the NS and the He WD, respectively.

In our work, the Ritter scheme is adopted to compute the mass-transfer rate (Ritter 1990). We have tested that the mass-transfer scheme has no significant influence on our results. Moreover, the isotropic re-emission model of mass transfer is also adopted (Tauris & van den Heuvel 2006). In this model, we assume that the material is transferred conservatively to the NS, and a fraction of this material, β is lost from the NS, taking away the specific orbital angular momentum of the NS. Here we adopt an accretion efficiency of 30% for the NS, i.e., $\beta = 0.70$ (Tauris & Savonije 1999; Antoniadis et al. 2012). Our results are basically independent of the NS accretion efficiency (Section 4.2), and also independent of the initial NS mass in the UCXB system (Section 4.5).

In addition, we assume that the accretion of the NS is limited by the Eddington mass-accretion rate given by the following expression:

$$\dot{M}_{\rm Edd} = \frac{4\pi\, G M_{\rm NS}}{\eta\, 0.20(1+X)c}, \quad (2)$$

where X is the hydrogen mass fraction of the accreted material. After the hydrogen shell of the He WD is removed, $X = 0$. We assume the ratio of gravitational mass to baryonic mass of accreted material to be 0.85, i.e., $\eta = 0.15$ (e.g., Lattimer & Prakash 2007). The inlist files for our simulations will be available on the Zenodo communities.[4]

[4] https://zenodo.org/communities/mesa?page=1&size=20

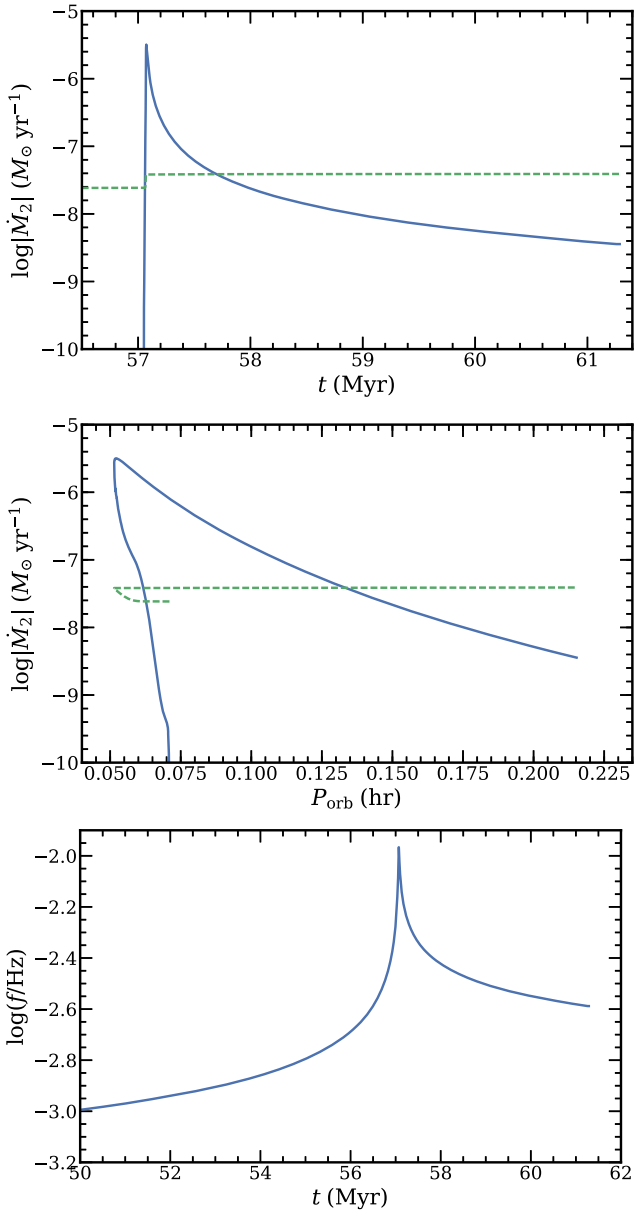

Figure 1. Example of the evolution of an NS+He WD UCXB. The initial binary parameters in this example are $M_2 = 0.25\,M_\odot$, $P_{\rm orb} = 0.05$ days. The upper and middle panels show the evolution of mass-transfer rate as a function of time and orbital period, respectively. The lower panel shows the evolution of GW frequency as a function of time. The dashed lines in the upper two panels indicate the Eddington accretion rate (which is not a constant due to the decrease in hydrogen in of the outer layer of the mass-losing WD).

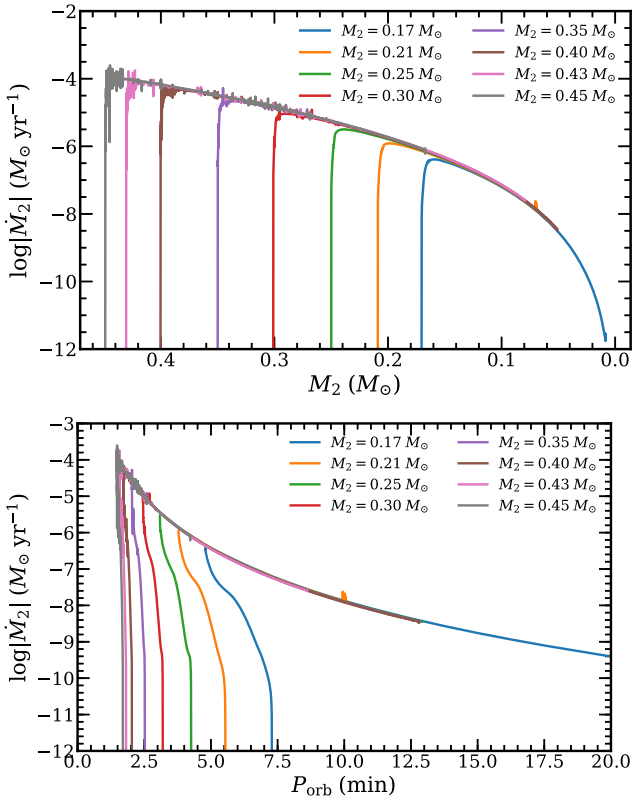

Figure 2. Evolution of mass-transfer rate as a function of WD mass (upper panel) and orbital period (lower panel) for NS+He WD binaries with different WD masses. The initial orbital periods and WD properties are listed in Table 1.

3. Results

3.1. An Example of UCXB Evolution

In Figure 1, we show an example of UCXB evolution of a NS+He WD system. The initial WD mass in this case is $0.25\,M_\odot$ and the initial orbital period is 0.05 days. During the initial detached phase, the binary separation decreases because of GW radiation and thus the GW frequency increases. At $t \simeq 5.7 \times 10^7$ yr, the WD fills its Roche lobe and initiates mass transfer. At the early stage of RLO, the orbital angular momentum loss due to GW radiation continues to dominate, leading to further increase of the GW frequency. When the orbital period reaches its minimum ($P_{\rm min} \sim 3.08$ minutes), the WD has lost its outer nondegenerate layer and the mass-transfer rate is close to its maximum value. Hereafter, the rate of orbital expansion dominates over the orbital decay due to GWs and the mass-transfer rate decreases with time. Consequently, the GW frequency also decreases as the orbit widens.

3.2. NS+He WD Binaries with Different WD Masses

In Figure 2, we present the evolution of mass-transfer rate as a function of WD mass and orbital period for a number of NS+He WD binaries with different WD masses. From this figure, we conclude that the maximum mass-transfer rate is larger for more massive WDs (as expected). Since massive WDs are more compact compared to lighter WDs, they initiate mass transfer at smaller orbital periods and reach smaller minimum orbital periods during RLO. The minimum orbital periods of these systems are between ∼1.5 and 4.8 minutes, see Table 1.

Our main result is that all NS+He WD binaries evolve with stable mass transfer and survive the UCXB phase. This is consistent with the semi-analytic results of some previous studies (e.g., Verbunt & Rappaport 1988; van Haaften et al. 2013), but the conclusion is very different from Bobrick et al. (2017), who find that only systems with He WD masses $<0.20\,M_\odot$ will undergo stable mass transfer in UCXBs by combining the results of hydrodynamic simulations with a semi-analytic long-term evolution model. This difference is likely due to the different assumptions of specific angular momentum loss in the different studies. Bobrick et al. (2017) (see their Figure 14) also found that the critical WD mass can be higher if they assumed that the mass loss from the systems takes away the specific angular momentum of the NS, as is the

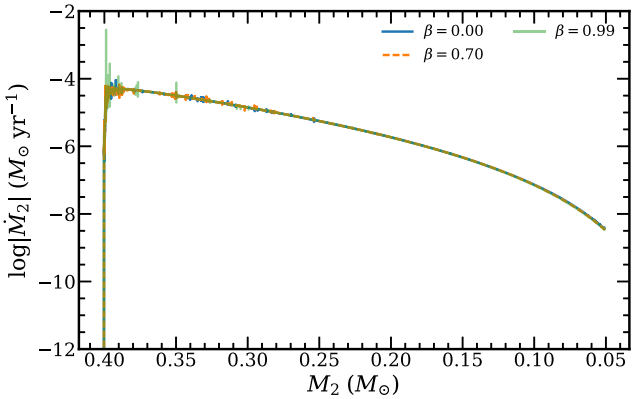

Figure 3. Comparison of mass-transfer rates for NS+He WD binaries with the same initial WD mass of 0.40 $M_\odot$, $M_{\rm NS} = 1.30\,M_\odot$, and $P_{\rm orb} = 0.02$ days , but different β-values of 0.00, 0.70, and 0.99, respectively.

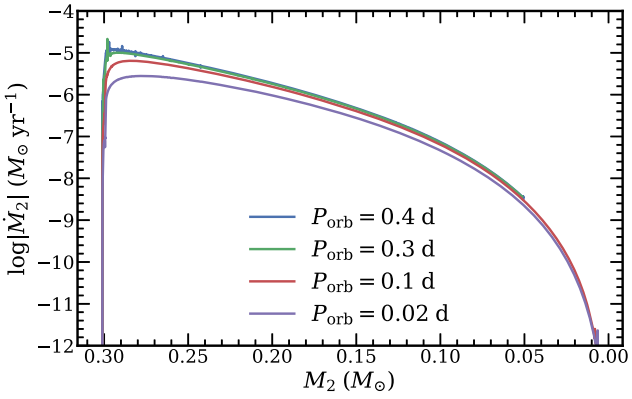

Figure 4. Comparison of mass-transfer rates for NS+He WD binaries with the same initial WD mass of 0.30 $M_\odot$, but different initial orbital periods of 0.40, 0.30, 0.10, and 0.02 days, respectively.

standard assumption in the isotropic re-emission model (Tauris & van den Heuvel 2006) applied in MESA.

Another interesting point in Figure 2 is that all the evolution tracks converge to a single branch after the mass-transfer rates reach their maximum, in agreement with the findings of Sengar et al. (2017).

4. Discussion

4.1. Influence of Accretion Disk

In our calculations, the effect of an accretion disk is not taken into account. van Haaften et al. (2012) carefully discussed this point and found that as long as the mass ratio, $q = M_2/M_{\rm NS} \gtrsim 0.01$, the torque between the outer disk and the WD donor star can efficiently transfer angular momentum back from the disk to the orbit. In this case, GW radiation and mass loss are the main orbital angular momentum loss mechanisms, which is consistent with our treatment. Only for $q \lesssim 0.01$, the feedback of angular momentum from the disk to the orbit is inefficient and the disk becomes a net sink of angular momentum. This will lead to a sudden increase of mass-transfer rate (see Figure 8 of van Haaften et al. 2012). Thus, we expect that our calculations at the very final stage, once $M_2 < 0.02\,M_\odot$, may not be reliable. It should be noted that as shown in Figure 2, only the model an initial WD mass of $0.17\,M_\odot$ was successfully evolved all the way to $0.008\,M_\odot$. The rest of the models terminated close to $\sim 0.05\,M_\odot$. However, it has been proposed that such systems may anyway become tidally disrupted (Ruderman & Shaham 1985) near this donor mass limit (possibly leading to production of isolated radio millisecond pulsars (MSPs) with planets, Martin et al. 2016).

4.2. Influence of NS Accretion Efficiency

The stability of our UCXB calculations are independent of the NS accretion efficiency. This is illustrated in Figure 3 where we have plotted three different computed tracks with $\beta = 0.0$ (fully conservative RLO), 0.70 and 0.99 (almost complete re-ejection of all transferred material), respectively. In all cases the initial WD mass, NS mass, and orbital period, were assumed to be $0.40\,M_\odot$, $1.30\,M_\odot$ and 0.02 days, respectively.

4.3. Influence of Initial Effective Temperature and Orbital Period

Aside from isolated binary star evolution, NS+He WD systems as UCXB sources may be produced from stable mass transfer after an episode of an exchange encounter event in a globular cluster, or they may form via the CE channel. Therefore, the effective temperature of the He WD at the onset of RLO can take a range of different values. In our calculations, we applied roughly the same central temperatures for all the different WD donors. However, if the initial orbital period is long (short) after the formation of the NS+He WD system (irrespective of its formation channel), the WD had long (short) time to cool down before initiating RLO. Thus, also the effective temperature of the WD (and thereby also its radius; Istrate et al. 2014b) at the onset of mass transfer can take a range of values. Therefore, the effect of different initial effective temperatures should be similar to the effect of different initial orbital periods.

To better understand the influence of initial effective temperature, we produced a $0.30\,M_\odot$ He WD with $T_{\rm eff} = 3.85 \times 10^4$ K (and a central temperature $\log(T_{\rm c}/{\rm K}) = 7.64$) using the method described in Section 2. We then compared the evolution of mass-transfer rate for NS+He WD binaries with different initial orbital periods. Our results are shown in Figure 4. We find that the mass-transfer rates are somewhat higher (up to one order of magnitude) for binaries with larger initial orbital periods. This is because these systems have longer WD cooling times and therefore become more degenerate. Except for this dissimilarity around the peak of mass-transfer rate, the difference between these binaries with different orbital periods is much less pronounced as the systems evolve further. We restricted our computations to binaries with initial orbital periods short enough to initiate the UCXB stage within the age of the Universe. As an example, the model with an initial orbital period of 0.40 days takes 12.26 Gyr to become semidetached. In addition to this, the time of the previous evolution before producing the NS+He WD binary should be added, which may also take several gigayears. Therefore, we do not consider binaries with longer orbital periods here.

4.4. GW Sources

Given the short orbital periods of UCXBs, they are strong GW emitters in the frequency band 1–10 MHz. Therefore, they are important GW sources for space-borne GW observatories

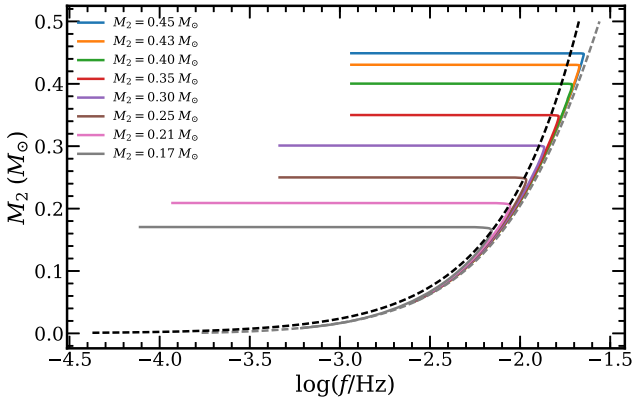

Figure 5. Evolution of donor mass as a function of GW frequency for NS+He WD binaries with different WD masses. The black and gray dashed lines indicate the analytic results of Equations (9) and (13), respectively.

like LISA (Amaro-Seoane et al. 2022), TianQin (Luo et al. 2016), and Taiji (Ruan et al. 2020).

In Figure 5, we show the evolution of WD mass as a function of GW frequency. It can be clearly seen that all evolutionary tracks converge to the same branch after the minimum orbital periods (maximum peak in frequencies) are reached. Therefore, there is a tight relation between the GW frequency and the WD mass for UCXBs detected in GWs. This relation can be understood as outlined in the following.

According to the Kepler's third law, the GW frequency (twice the orbital frequency) is given by

$$f = \frac{2}{P_{\rm orb}} = \frac{1}{\pi}\sqrt{\frac{G(M_{\rm NS}+M_2)}{a^3}}, \tag{3}$$

where $P_{\rm orb}$ is the orbital period; $M_{\rm NS}$ and M_2 are the NS mass and He WD mass, respectively; and a is the binary separation. The Roche-lobe radius of the He WD can be estimated with the following equation (Paczyński 1971):

$$\frac{R_{\rm rl}}{a} \simeq 0.462\left(\frac{M_2}{M_{\rm NS}+M_2}\right)^{1/3}, \tag{4}$$

which is a good approximation for $M_2/M_{\rm NS} < 0.523$ (and therefore all UCXBs), and where $R_{\rm rl}$ is the Roche-lobe radius of the He WD. During the mass-transfer phase, the radius of He WD (R_2) equals that of its Roche lobe:

$$R_2 = R_{\rm rl}. \tag{5}$$

For a relation between WD mass and radius, we may at first apply (Chandrasekhar 1939)

$$R_2 = 0.013\,R_\odot\left(\frac{M_2}{M_\odot}\right)^{-1/3}. \tag{6}$$

Combining Equations (3)–(6), we obtain

$$f = C_1\,M_2, \tag{7}$$

where the constant C_1 is given by

$$C_1 = \frac{1}{\pi}\sqrt{\frac{(0.462)^3\,G}{(0.013\,R_\odot)^3 M_\odot}} = 2.13\times10^{-35}\ {\rm Hz\ g^{-1}}. \tag{8}$$

Rewriting in more convenient units, we finally obtain

$$f = 4.23\ {\rm MHz}\left(\frac{M_2}{0.1\,M_\odot}\right). \tag{9}$$

It is interesting to note that the GW frequency, f is *independent* of the accreting NS mass and only depends on the He WD mass, M_2.

Alternatively, applying a slightly more accurate WD mass–radius relation, first proposed by Peter Eggleton and quoted in Verbunt & Rappaport (1988):

$$R_2 = 0.0114\,R_\odot\left[\left(\frac{M_2}{M_{\rm Ch}}\right)^{-2/3} - \left(\frac{M_2}{M_{\rm Ch}}\right)^{2/3}\right]^{1/2} \times\left[1+3.5\left(\frac{M_2}{M_p}\right)^{-2/3}+\left(\frac{M_2}{M_p}\right)^{-1}\right]^{-2/3}, \tag{10}$$

where $M_{\rm Ch}\simeq 1.44\,M_\odot$ is the Chandrasekhar mass limit for a WD and $M_p = 0.00057\,M_\odot$ is a constant, we find

$$f = C_2\,M_2^{1/2}\times\left[\left(\frac{M_2}{M_{\rm Ch}}\right)^{-2/3} - \left(\frac{M_2}{M_{\rm Ch}}\right)^{2/3}\right]^{-3/4} \times\left[1+3.5\left(\frac{M_2}{M_p}\right)^{-2/3}+\left(\frac{M_2}{M_p}\right)^{-1}\right] \tag{11}$$

where the constant C_2 is given by

$$C_2 = \frac{1}{\pi}\sqrt{\frac{(0.462)^3\,G}{(0.0114\,R_\odot)^3}} = 1.16\times10^{-18}\ {\rm Hz\ g^{-1/2}}, \tag{12}$$

or rewritten in more convenient units:

$$f = 16.3\ {\rm MHz}\left(\frac{M_2}{0.1\,M_\odot}\right)^{1/2} \times\left[\left(\frac{M_2}{M_{\rm Ch}}\right)^{-2/3} - \left(\frac{M_2}{M_{\rm Ch}}\right)^{2/3}\right]^{-3/4} \times\left[1+3.5\left(\frac{M_2}{M_p}\right)^{-2/3}+\left(\frac{M_2}{M_p}\right)^{-1}\right]. \tag{13}$$

Considering that the bulk of detectable LISA sources are found where the detector has its highest sensitivity (near 5 MHz), we can rewrite the expression in the limit where $M_2\sim 0.1\,M_\odot$ and we obtain here

$$f \simeq 4.89\ {\rm MHz}\left(\frac{M_2}{0.1\,M_\odot}\right)^{1/2}. \tag{14}$$

In Figure 5, we have plotted the expressions from Equations (9) and (13) as dashed lines and they are found to be quite consistent (especially Equation (13)) with the models from the MESA calculations. As a bonus of the independence of the frequency on NS mass, the WD mass can be directly inferred from observations of UCXBs by only measuring the GW frequency.

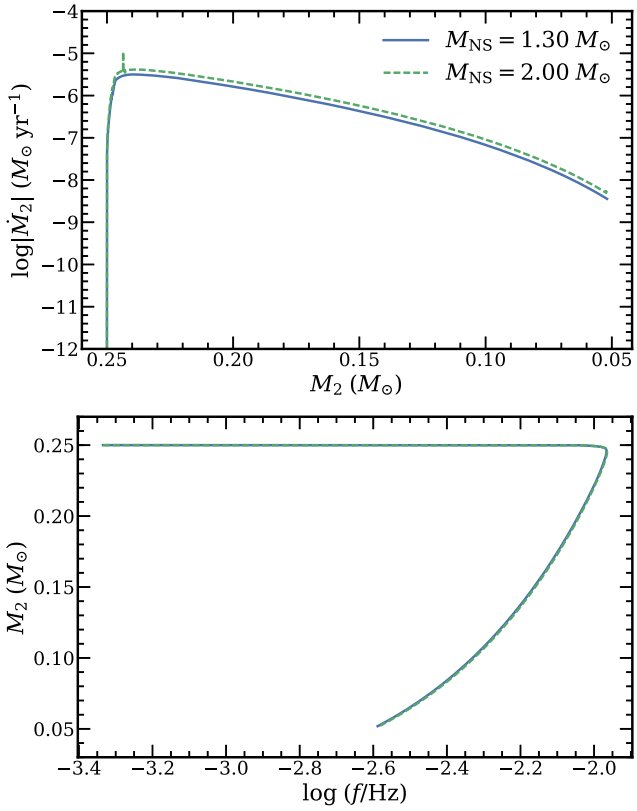

Figure 6. Comparison of the evolution of NS+He WD UCXBs with different initial NS masses. The initial donor star masses (and temperatures) and orbital periods of these two models are the same ($0.25\,M_\odot$ and 0.05 days, respectively). The upper panel shows the evolution of mass-transfer rate as a function of decreasing donor mass. The lower panel shows the evolution of donor WD mass as a function of GW frequency. The blue solid and green dashed lines are for the two models with an initial NS mass of 1.30 and $2.0\,M_\odot$, respectively.

4.5. Influence of Initial NS Mass

To further investigate the influence of the NS mass on the general UCXB evolution, we computed a NS+He WD model with an initial NS mass of $2.0\,M_\odot$, an initial He WD mass of $0.30\,M_\odot$ and an initial orbital period of 0.05 days. In Figure 6, we compare this model directly to a similar model with an initial NS mass of $1.30\,M_\odot$. From the two panels of this figure, we conclude that the influence of initial NS mass on the general UCXB evolution is very limited.

4.6. Hydrogen Abundance in UCXBs

Given that He WDs are produced with an outer layer of residual hydrogen (H) from the LMXB stage, we expect that H could be present in the accretion disk of UCXBs in their early phases. In Figure 7, we present the evolution of surface H abundance and mass of the He WD donors as a function of time for models with initial He WD masses of 0.17, 0.21, 0.30, and $0.40\,M_\odot$. From this plot, we see that H is only expected to be present in the accretion disk of an UCXB at its very early stage of the mass transfer, lasting for about 10^3–10^5 yr. Given this short time interval, it will be difficult to observe the presence of H in the accretion disk.

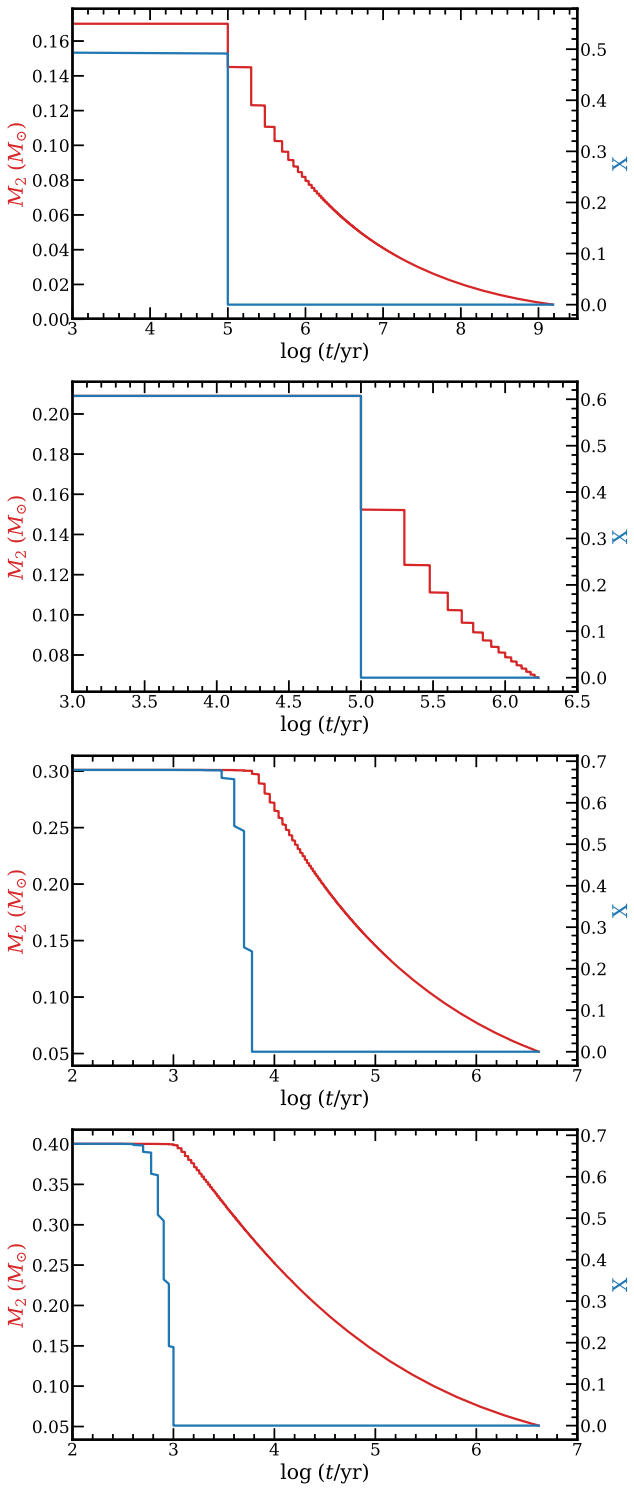

Figure 7. Evolution of surface H abundance (blue lines) and WD mass (red lines) as a function of time for UCXBs with different initial WD masses. From top to bottom, the initial WD masses are 0.17, 0.21, 0.30, and $0.40\,M_\odot$, respectively. The $t = 0$ point indicates the onset of mass transfer ($\log(\dot{M}_2/(M_\odot/{\rm yr})) >= -12.0$). The left and right y-axes indicate WD mass and surface H abundance, respectively.

5. Conclusion

With the stellar evolution code MESA, we modeled the evolution of NS+He WD binaries with WD masses ranging from $0.17\,M_\odot$–$0.45\,M_\odot$. The main results are as follows:

1. All NS+He WD binaries (with an initial WD mass anywhere in the interval between ∼0.17 and 0.45 $M_\odot$) undergo *stable* UCXB mass transfer. This is a prediction that is, in principle, easily testable with LISA, TianQin, and Taiji GW observations, although population synthesis is needed to reveal how many systems are detectable, given that the WD mass initially decreases rapidly.
2. The larger the WD masses, the larger the maximum mass-transfer rates, and the smaller the minimum orbital periods of the NS+He WD systems. The minimum orbital periods range between 1.5 and 4.7 minutes, corresponding to maximum GW frequencies of $f \approx$ 7.1–22 MHz.
3. There is a tight correlation between WD mass and GW frequency for NS+He WD UCXBs, *independent* of NS mass. With the relation in Equation (13) (or Equation (9)), the WD mass can be inferred in all such UCXBs for which the GW frequency can be determined from observations. A measurement of the chirp mass, $\mathcal{M}(f, \dot{f}) \equiv (M_1 M_2)^{3/5}/(M_1 + M_2)^{1/5}$, will thus directly provide the NS mass.
4. It is very unlikely that hydrogen will be detected in the accretion disk of UCXBs with a He WD donor star because their residual outer layer of hydrogen ($\lesssim$0.01 $M_\odot$, left from the detached LMXB progenitor system) is removed within 10^5 yr.

We thank the anonymous referee for comments that helped improve the manuscript. This work is partially supported by the National Key R&D Program of China (grant Nos. 2021YFA1600400/401, 2021YFA1600403), the National Natural Science Foundation of China (grant Nos. 12090040/12090043, 12073071, 11873016, 11733008), Yunnan Fundamental Research Projects (grant Nos. 202001AT070058, 202101AW070003), the science research grants from the China Manned Space Project with No. CMS-CSST-2021-A10) and Youth Innovation Promotion Association of Chinese Academy of Sciences (grant No. 2018076). The authors gratefully acknowledge the "PHOENIX Supercomputing Platform" jointly operated by the Binary Population Synthesis Group and the Stellar Astrophysics Group at Yunnan Observatories, CAS. We are grateful to the MESA council for the MESA instrument papers and website.

Software: MESA (Paxton et al. 2011, 2013, 2015, 2018, 2019).

ORCID iDs

Thomas M. Tauris https://orcid.org/0000-0002-3865-7265
Zhanwen Han https://orcid.org/0000-0001-9204-7778

References

Amaro-Seoane, P., Andrews, J., Arca Sedda, M., et al. 2022, arXiv:2203.06016
Antoniadis, J., van Kerkwijk, M. H., Koester, D., et al. 2012, MNRAS, 423, 3316
Bobrick, A., Davies, M. B., & Church, R. P. 2017, MNRAS, 467, 3556
Bobrick, A., Zenati, Y., Perets, H. B., Davies, M. B., & Church, R. 2022, MNRAS, 510, 3758
Chandrasekhar, S. 1939, An Introduction to the Study of Stellar Structure (Chicago, IL: Univ. Chicago Press)
Chen, H.-L., Tauris, T. M., Han, Z., & Chen, X. 2021, MNRAS, 503, 3540
Fernández, R., Margalit, B., & Metzger, B. D. 2019, MNRAS, 488, 259
Istrate, A. G., Marchant, P., Tauris, T. M., et al. 2016, A&A, 595, A35
Istrate, A. G., Tauris, T. M., & Langer, N. 2014a, A&A, 571, A45
Istrate, A. G., Tauris, T. M., Langer, N., & Antoniadis, J. 2014b, A&A, 571, L3
Ivanova, N., Heinke, C. O., Rasio, F. A., Belczynski, K., & Fregeau, J. M. 2008, MNRAS, 386, 553
Ivanova, N., Justham, S., Chen, X., et al. 2013, A&ARv, 21, 59
Katz, J. I. 2021, MNRAS, 508, L12
King, A., Olsson, E., & Davies, M. B. 2007, MNRAS, 374, L34
Landau, L. D., & Lifshitz, E. M. 1971, The Classical Theory of Fields (Oxford: Pergamon)
Lattimer, J. M., & Prakash, M. 2007, PhR, 442, 109
Luo, J., Chen, L.-S., Duan, H.-Z., et al. 2016, CQGra, 33, 035010
Martin, R. G., Livio, M., & Palaniswamy, D. 2016, ApJ, 832, 122
Nelson, L. A., Rappaport, S. A., & Joss, P. C. 1986, ApJ, 304, 231
Paczyński, B. 1971, ARA&A, 9, 183
Paschalidis, V., Liu, Y. T., Etienne, Z., & Shapiro, S. L. 2011, PhRvD, 84, 104032
Paschalidis, V., MacLeod, M., Baumgarte, T. W., & Shapiro, S. L. 2009, PhRvD, 80, 024006
Paxton, B., Bildsten, L., Dotter, A., et al. 2011, ApJS, 192, 3
Paxton, B., Cantiello, M., Arras, P., et al. 2013, ApJS, 208, 4
Paxton, B., Marchant, P., Schwab, J., et al. 2015, ApJS, 220, 15
Paxton, B., Schwab, J., Bauer, E. B., et al. 2018, ApJS, 234, 34
Paxton, B., Smolec, R., Schwab, J., et al. 2019, ApJS, 243, 10
Ritter, H. 1990, in IAU Coll. 122, Physics of Classical Novae, ed. A. Cassatella & R. Viotti (Berlin: Springer Verlag), 313
Ruan, W.-H., Guo, Z.-K., Cai, R.-G., & Zhang, Y.-Z. 2020, IJMPA, 35, 2050075
Ruderman, M. A., & Shaham, J. 1985, ApJ, 289, 244
Sengar, R., Tauris, T. M., Langer, N., & Istrate, A. G. 2017, MNRAS, 470, L6
Tauris, T. M. 2018, PhRvL, 121, 131105
Tauris, T. M., & Savonije, G. J. 1999, A&A, 350, 928
Tauris, T. M., & van den Heuvel, E. P. J. 2006, Compact Stellar X-ray Sources, Vol. 39 (Cambridge: Cambridge Univ. Press), 623
Tauris, T. M., & van den Heuvel, E. P. J. 2023, Physics of Binary Star Evolution (Princeton, NJ: Princeton Univ. Press)
Tutukov, A. V., & Yungelson, L. R. 1993, ARep, 37, 411
van Haaften, L. M., Nelemans, G., Voss, R., et al. 2013, A&A, 552, A69
van Haaften, L. M., Nelemans, G., Voss, R., Wood, M. A., & Kuijpers, J. 2012, A&A, 537, A104
Verbunt, F., & Rappaport, S. 1988, ApJ, 332, 193
Yu, S., Lu, Y., & Jeffery, C. S. 2021, MNRAS, 503, 2776
Yungelson, L. R., Nelemans, G., & van den Heuvel, E. P. J. 2002, A&A, 388, 546
Zenati, Y., Bobrick, A., & Perets, H. B. 2020, MNRAS, 493, 3956
Zenati, Y., Perets, H. B., & Toonen, S. 2019, MNRAS, 486, 1805